2019 SECED Conference
Earthquake risk and engineering towards a resilient world
9-10 September 2019, Greenwich, London

POUNDING IN NEPALESE SCHOOL BUILDINGS.

Ted CROSS[1], Flavia DE LUCA[1], Raffaele DE RISI[1], Tek RAJ RANA[2], Tim MITCHELL[2] & Alan SWEETMAN[2]

Abstract: *The seismic performance of a two storey RC school in Nepal is assessed using non-linear time history analysis (NLTHA). The school was constructed by Pahar Trust and utilizes a seismic gap to avoid issues caused by the torsional effect of the off centre stair case. A fibre model the of RC structure is implemented in finite element (FE) open-source software OpenSees, where NLTHA is employed to assess the seismic performances under different input motions. In particular, three sets of accelerograms are selected: (i) recorded waveforms of the 2015 Gorkha earthquake, (ii) a code-compatible selection compliant with pre-Gorkha earthquake probabilistic seismic hazard analysis (PSHA), (iii) a code-compliant selection compatible with post-Gorkha PSHA. The inter-storey drift demand and the effectiveness of the seismic gap is then assessed. The inter-storey drift values are used to verify the performances of the school against Eurocode 8 capacity limit. The seismic gap provides adequate clearance to avoid pounding when the structure is exposed to the Gorkha ground motions and life safety limit state (10% probability is 50 years) motions for pre-Gorkha PSHA. The structure exhibits pounding with a small number of the post-Gorkha ground motions. A fragility curve for pounding is finally obtained for the school using Cloud Analysis linear regression approach.*

Introduction

Nepal seismic hazard

Nepal sits on the most active segment of the Main Himalayan Thrust (MHT) (Ram and Wang, 2013). Kathmandu sits in a fluvio-lacustrine basin with 500-600m deep deposits of loose unconsolidated clay, silts, sand and gravel sediments (Mugnier et al., 2011). These loose deposits cause the amplification of long period ground motions (Paudyal et al., 2012) as shown during the 2015 Gorkha earthquake (Rupakhety et al. 2017).

Major earthquakes have been reported in Kathmandu valley in 1255, 1408, 1505, 1833, 1934 and 2015 each with a magnitude over 7.5 (Ram and Wang, 2013). The 2015 Gorkha earthquake had a moment magnitude of Mw 7.8 and the epicentre was 80 km west – northwest of Kathmandu. This earthquake caused 9,000 deaths, 25,000 injuries and more the 6,000 schools collapsed. 60% of central Nepalese villages are located on near-threshold or threshold dip slopes further increasing exposure of schools (Catlos et al., 2016; Ghimire and Parajuli, 2016).

Probabilistic seismic hazard analysis (PSHA) is the reference approach for the estimation of intensity of earthquakes for design purposes. Due to seismic data only being accurately collected for the last 50-60 years (Mulargia et al., 2017), there is insufficient data to create an accurate PSHA and this leaves the PSHA susceptible to change when a large earthquake occurs, and new evidence is available.

Prior to the 2015 Gorkha earthquake the design earthquake (10% probability of occurrence in 50 years) for Kathmandu had a peak ground acceleration (PGA) of 0.38g (e.g., Chaulagain et al., 2015). Subsequent to the Gorkha earthquake several new PSHA studies have been carried out for the Kathmandu valley and have put the PGA for the design earthquake above 0.60g due to a new modelling approach of the Main Himalayan Trust based on physical evidence and new global Ground Motion Prediction Equations (Stevens, et al., 2018; Pokhrel et al. 2019).

[1] University of Bristol, Bristol, United Kingdom, tc14527@bristol.ac.uk
[2] Pahar Trust, Pokhara, Nepal

Pahar Trust

Pahar Trust is a UK based charity established in 1991 which aims to improve education, sanitation and health in rural Nepal, furthermore they aim to remove barriers to education in these communities and make education as inclusive as possible (Pahar-trust.org, 2019). Pahar Trust was founded by Tom Langridge MBE and Chandra Bahadur Gurung, both former Queens Gurkha Engineers. They construct 4-6 reinforced concrete (RC) schools per year with many of them using the same design as in Nepal all school designs need to be approved by the Department of Education and having an adaptable design to be employed in multiple cases can reduce significantly the design and construction cost of the schools. One of the approved RC design "templates" has six class rooms across two storeys, two examples of where this design has been implemented is Shree Himalaya, Mauja, Kaski and Shree Ramkot Secondary School (see Figure 1).

a) b)

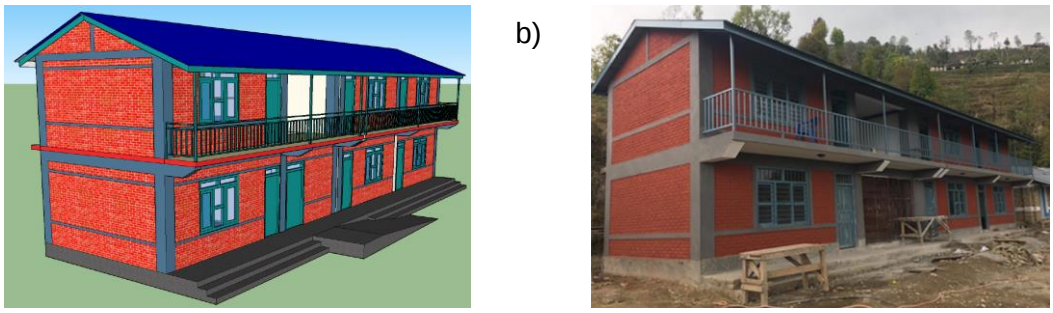

Figure 1. Pahar Trust sample school (a) Architectural drawing (Pahar Trust, 2019) *(b) Example project (Shree Himalaya, Mauja, Kaski)* (Pahar-trust.org, 2019).

Sample school

The template school is 5.8 m tall, 4.9 m deep and 20.3 m long. It is four by one bay and has a 102 mm (4 inch) seismic gap in the middle. The school is a reinforced concrete frame with masonry façade. The school has a reinforced concrete slab with a dogged type staircase where the waist slab is supported by a masonry wall. Due to this staircase being off centre there is an asymmetrical design which would lead to torsion, this is addressed by implementing a seismic gap in the building (Pahar Trust, 2019), as shown in Figure 2. Figure 3 shows the sections for the beams, the "at support" reinforcement is applied for 1676 mm in B1 and for 1600 mm in B2 as to ensure capacity design.

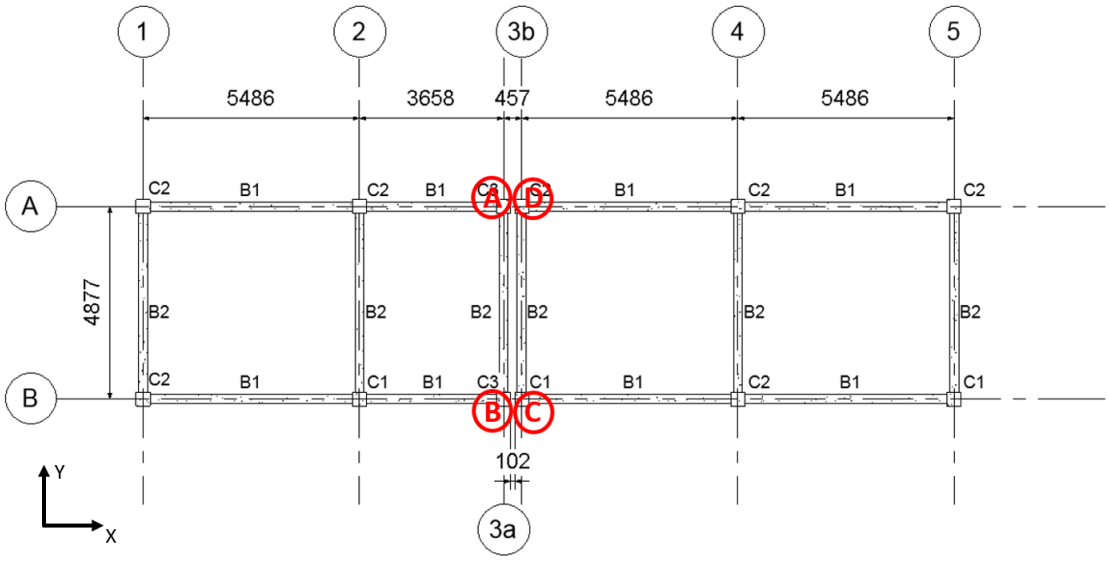

Figure 2. Beam and column layout of Pahar trust template school.

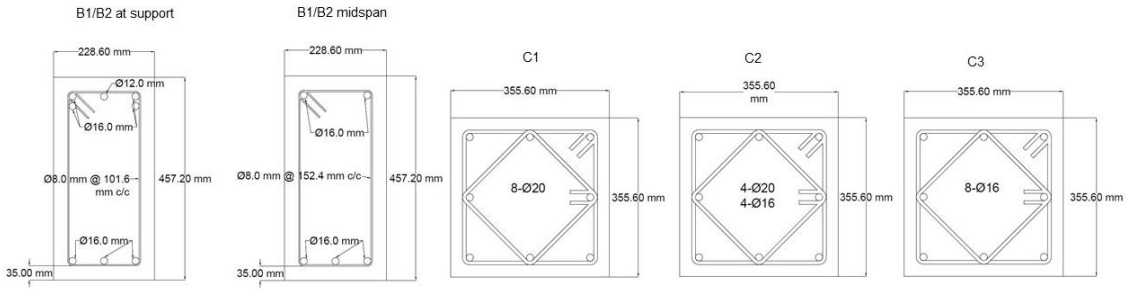

Figure 3. Beam and column section properties

Pounding

Pounding is defined as collisions that occur between adjacent buildings during an earthquake and has been identified as one of the main causes of structural damage during an earthquake (Karayannis and Favvata, 2004). Despite modern codes requiring adequate separating distance between adjacent buildings, structural pounding occurs for four main reasons: (i) sometimes the suggested separation does not account for modern construction techniques that allow large displacements due to an inelastic response; (ii) high cost of land in densely populated cities; (iii) errors in selection and interpretation of seismic hazard and (iv) structures designed in accordance with outdated codes where minimum separation gap had not been provided (Favvata, 2017).

Structural pounding occurs in two main types: slab-to-slab and slab-to-column. Slab-to-column is considered to be significantly more severe as the shear load to the column can cause localized failure which can lead to progressive global collapse (Skrekas et al. 2014). The template school in this paper should only be susceptible to slab-to-slab pounding as the floor slabs are at the same level. There are four main factors that affect the pounding of two structures, these are; (i) the separation distance; (ii) the height of the structures; (iii) the period of the structure (higher period pounding more likely) and (iv) different periods for adjacent buildings (this causes out of phase vibrations) (Lin and Weng, 2001).

School model

Overview

A non-linear finite element (FE) model of the template school was implemented in the open source program OpenSees. A fibre model was used for the RC sections and the plastic hinges were implemented using the “Hinge Radau” function in OpenSees which uses two-point Gauss-Radau integration over the hinge. This function is implemented in OpenSees (Scott et al. 2006) and the plastic hinge lengths were calculated in accordance with Eurocode 8 (EN 1998-1, 2004). Two rigid diaphragms are assumed at both the first-floor level and the roof level for the two buildings composing the school. The stairs were implemented in the FE model using a member with cross sectional properties that are equal to the cross-sectional properties of the stairs. This member extends from the node supporting the stairs to the floor node that is closest to the landing area of the stairs, a technique suggested by Fardis (2009).

Material properties

It was not specified the grade of concrete used in the construction of these schools so an assumed grade of C25/30 is used giving a corresponding mean compressive strength of 33 MPa and elastic modulus of 31,476 MPa (EN 1992-1-1, 2004) was used for the unconfined concrete.

The strength of the confined concrete was calculated using the Kent and Park model (1971) that was modified (Park et al., 1982) to account for the additional strength of the concrete due to the confining concrete. This modifies the unconfined compressive strength by a factor K as shown in equation 1 where f'_c is the peak stress reached in the unconfined concrete and f''_c is the peak stress reached in the confined concrete.

$$f''_c = Kf'_c \quad (1)$$

The factor K is calculated using equation 2 where ρ_s is the ratio of the volume of the confining steel to the volume of the concrete core and f_{yh} is the yield stress of the confining steel.

$$K = 1 + \frac{\rho_s f_{yh}}{f'_c} \quad (2)$$

This results in a unique confined concrete compressive strength for each section as the ratio of confining steel varies in each section.

SteelMPF was used for the material properties of the steel rebar. This material uses the hysteretic model developed by Menegotto and Pinto (1973) and further modified by Filippou et al. (1983). This model was implemented into Opensees by Kolozvari et al. (2015). It is specified in the design of the structure that steel grade is Fe 500 hence a yield strength of 500 MPa is used and an elastic modulus of 200 GPa is used in accordance with Eurocode 2 (EN 1992-1-1, 2004).

Assessment of structural performances

Modal properties

For the modes of the building the building can be considered as two separate structures as the structures at either side of the seismic gap to not interact. Table 1 shows the first six periods of each structure where structure 1 is the structure that contains the staircase. It can be seen that structure 1 has lower fundamental periods due to the additional stiffness offered by the staircase.

	Structure 1 (with staircase)	**Structure 2**
Mode 1 (s)	0.229	0.242
Mode 2 (s)	0.216	0.237
Mode 3 (s)	0.202	0.217
Mode 4 (s)	0.077	0.082
Mode 5 (s)	0.074	0.080
Mode 6 (s)	0.070	0.074

Table 1. Modal properties of structures.

Ground motion selection

This analysis was carried out using three ground motions suites. The first group of ground motions (ground motion set 1) is detailed in Table 3 in the appendix. This contains five available recordings of the 2015 Gorkha earthquake (Rupakhety et al. 2017). The elastic response spectrum of these motions is shown in Figure 4 where is can be seen there is significant amplification in the spectral acceleration in the large period range (1s-6s), this is due to basin effects caused by the loose fluvio-lacustrine deposits and source effects of the Gorkha earthquake (Rajaure et al., 2016). KTP is not affected by basin effects as it is situated on a rock outcrop near the western basin edge.

The second ground motion suite (ground motion set 2) is selected from the NGA-west 2 database and is compatible with Eurocode 8 type 1 spectral shape for soil class C (predominant in the Kathmandu valley) anchored at 0.38g (see Figure 5a). Importance class 1.0 is used. The PGA value of 0.38g is used as it is the 10% in 50 years exceedance value for PSHA studies carried out before the Gorkha earthquake (e.g., Chaulagain et al., 2015), in the following referred as “pre-Gorkha” PSHA. 11 couples of ground motions are used, no scaling is used and none of the motions are pulse like motions. The spectrum matching was done in accordance with Eurocode 8 (EN 1998-3, 2005) whereby between 0.2T1 and 2.0T1, the arithmetic mean of the 5% damped elastic response spectrum is at no point lower than 90% of the design spectrum.

The third ground motion suite (ground motion set 3, in the following referred as “post-Gorkha”) uses the same ground motions as the previous set but multiplied by an additional scaling factor of 1.579 resulting in a PGA of 0.60g which has been obtained from a post-Gorkha PSHA (Stevens et al., 2018), see Figure 5b. The scale factor for the ground motions should not exceed specific maximum values to avoid bias in the results; this limit varies from 2 to 4 (Bommer and Acevedo, 2004).

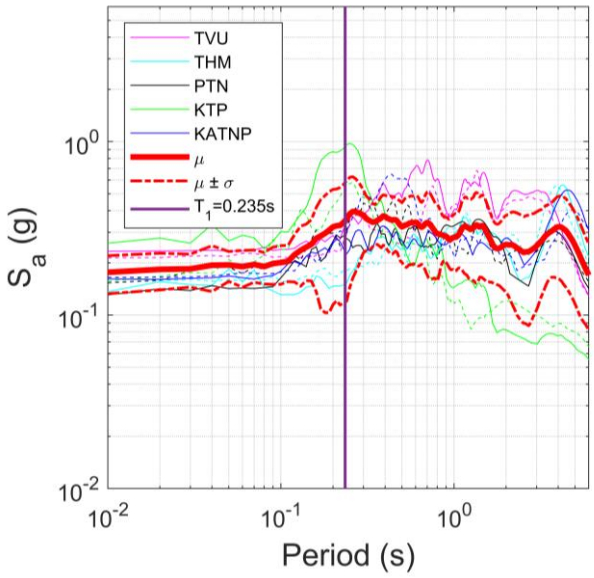

Figure 4. 5% damped elastic response spectrum for Gorkha 2015 ground motions

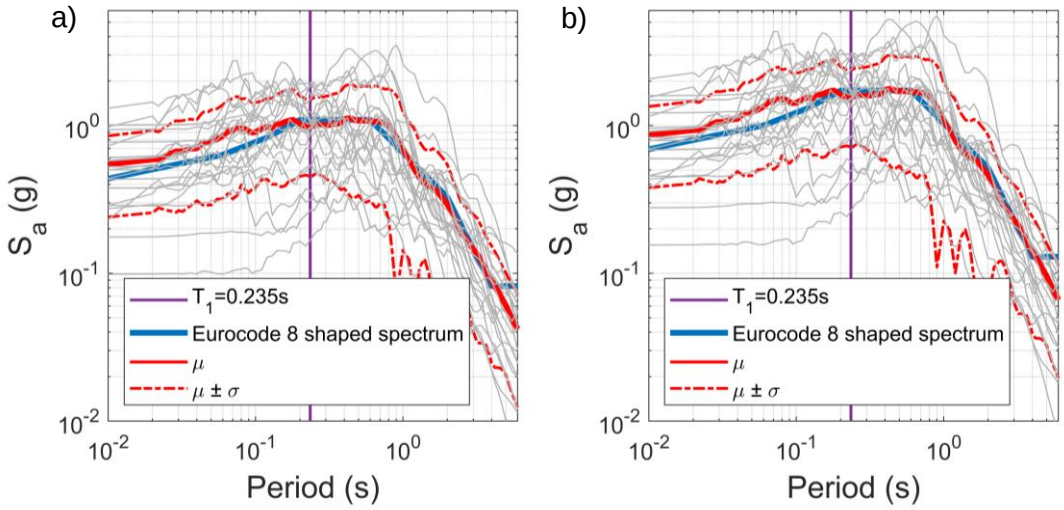

Figure 5. 5% damped elastic response spectrum for (a) EC 8 compliant (pre-Gorkha PSHA) motions (b) EC 8 compliant (post-gorkha PSHA) motions.

Results

Nonlinear Static Analysis

Static Pushover (SPO) analysis is carried out as to assess the strength and deformation characteristics of the structure. A lateral load pattern which is in accordance with Eurocode 8 (EN 1998-1, 2004) *as shown in equation 3 where F_b is the base shear, z_i is the height of the storey and m_i is the mass of the respective storey.*

$$F_i = F_b \frac{z_i m_i}{\sum z_j m_j} \tag{3}$$

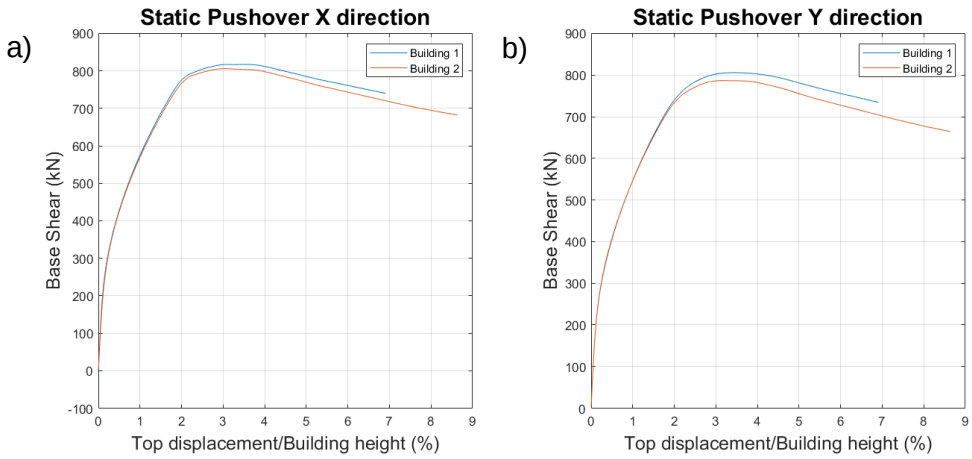

Figure 6. Static Pushover Analysis results (a) Building 1 (with staircase) (b) Building 2

The deformed shape of the static pushover analysis shows a soft storey mechanism occurring across the first storey of the building. The peak base shear was verified by calculating the moment resistance of the column section.

Non-linear Time History

Non-linear time history is carried out with each of the 27 pairs of ground motions. Each set was run twice, swapping the two components along the two prinicipal directions of the buildings. This gives a total of 54 analysis. Figure 7 shows the displacement of the top of building 1 for the ground motion giving the largest displacement in each set. For the Gorkha ground motion set this was the KTP recording and for the spectrum compatible sets the Tottori recording is shown. It can be seen that the post-Gorkha ground motion results in a significantly larger displacement due to the non-linear response of the structure and it shows a significant residual dispacement with respect to the maximim response obtained with the pre-Gorkha set. The Gorkha record does not show any residual dispacement.

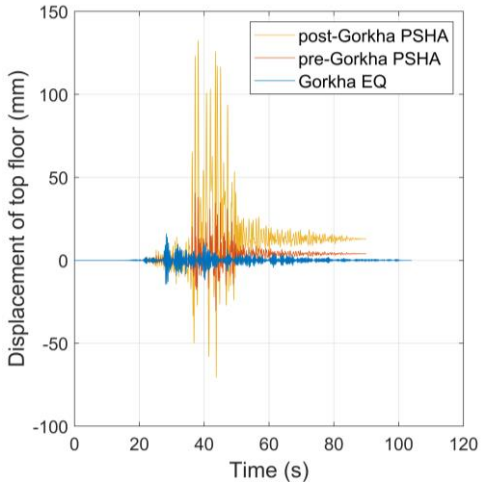

Figure 7. The displacement of the top of the structure in response to pre-Gorkha, post-Gorkha and Gorkha earthquakes.

Interstorey Drift Ratio

The results from the non-linear time history analysis are used to find the interstorey drift ratio (IDR) for each of the buildings, this data is summarized in Figure 8. It is shown in Figure 8 that the median IDR for the pre-Gorkha PSHA ground motion set is 0.59% for Building 1 and 0.70% for Building 2 which exceeds the Eurocode threshold for nonstructural brittle elements (EN 1998-1 2004) employed for the damage limitation limit state.

The post-Gorkha ground motion set gave a median IDR of 1.58% which significantly exceeds the threshold for non-structural brittle elements. It can be seen that there is a significantly larger variation in the spectrum compatible ground motion sets, this is due to the Gorkha ground motion set not having inter-event variability (i.e., one single event versus 11 different events).

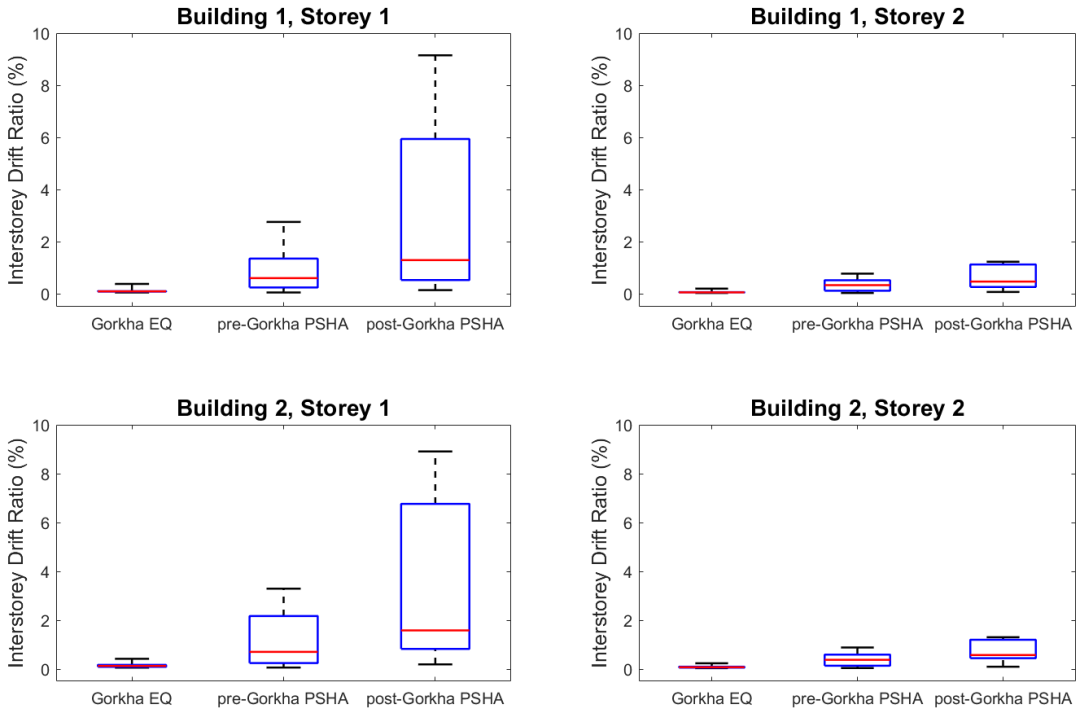

Figure 8. The distribution of peak interstorey levels for each ground motion set.

Pounding

Pounding occurs when the displacement between point A and point D or point B and point C, as depicted on Figure 2, is less than zero. For each ground motion the closest distance relevant for pounding is recorded and plotted in Figure 10. This is calculated as shown in Figure 9 using equation 4, displacement in x direction (see Figure 2) is always positive. P is the distance between the two structures (i.e., 102 mm in the case of the Pahar Trust school).

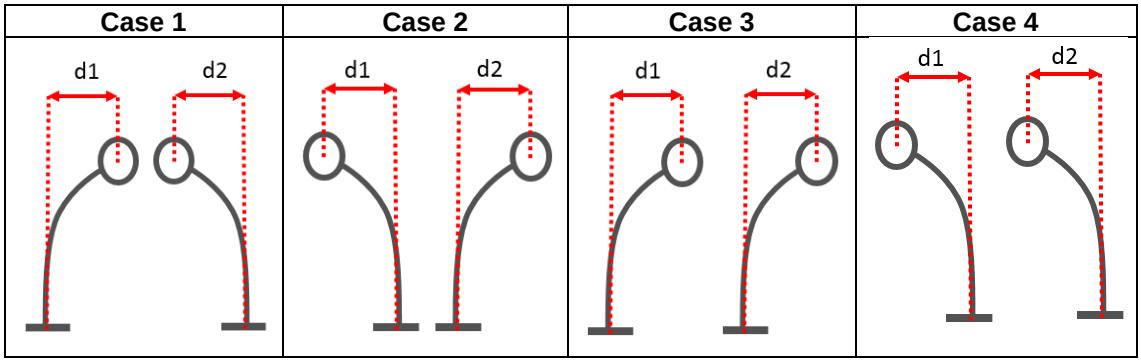

Figure 9. Four possible displacement scenarios for pounding.

$$\boldsymbol{max(d_1 - d_2) > P} \tag{4}$$

Due to the non-linear response of the structure significantly larger displacement occurs when the ground motions are scaled up for the post-Gorkha suite (Figure 5b). Pounding occurs for three ground motions in the post-Gorkha suite as shown in Figure 10.

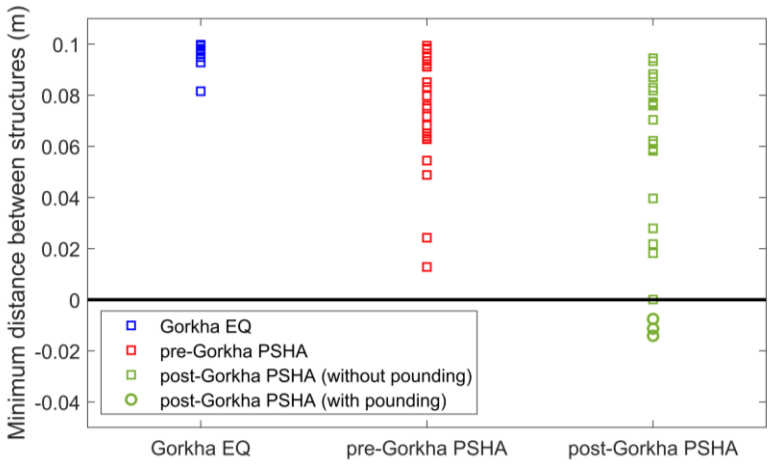

Figure 10. Minimum distance between adjacent structures.

From figure 10 it can be seen that with the Gorkha ground motion set that no pounding occurred and the closest point to pounding was 81 mm which occurred during the KTP ground motion recording. It can be seen in figure 4 that KTP has the largest spectral acceleration at 0.235s as it is situated on rock. From this we can conclude that the site effects in the Kathmandu basin caused Pahar schools to be less likely exhibit pounding, in the 2015 earthquake.

The pre-Gorkha PSHA ground motion set is significantly closer to pounding, with the Tottori ground motion being 12 mm from pounding, however no pounding occurs. The closest point to pounding is during the Tottori ground motion, this ground motion has a spectral acceleration that is significantly higher than the mean, however it is not the highest in the ground motion set. This is due to the building being more out of phase in the Tottori analysis.

The post-Gorkha PSHA ground motion set is significantly closer to pounding with 3/22 of the ground motions exhibiting pounding. It can be seen that the pounding goes up by more than a factor 1.58, as the ground motion is scaled by. This is due to the non-linear response of the structure. Pounding occurs within one standard deviation of the mean which indicates that in a typical ground motions selection compatible with Eurocode 8 spectra and using a post-Gorkha PSHA will exhibit pounding.

Fragility

For pounding a specific fragility curve can be obtained using the linear regression approach for cloud analysis (Jalayer et al., 2015) and assuming the spectral acceleration at the fundamental period of the structure. Considering that pounding affects two buildings, the reference period is the average of the fundamental period along x direction for building 1 and 2 (see figure 2) and it equals to 0.235s. This is considered to be the most suitable choice as intensity measure for this fragility curve.

The linear regression is shown in Figure 11a and the resulting fragility curve is shown in Figure 11b. The fragility curve in Figure 11b gives the cumulative probability function for the occurrence of damage of the buildings because of pounding recorded at the top storey of the school. It can be observed that the designed seismic gap of 102 mm provides a safe solution against pounding with a 50% probability of occurrence for a spectral acceleration value of 2.7g. Further analyses are needed to validate this result as the use of the scaling of the same records for pre-Gorkha and post-Gorkha suite can introduce bias in the fragility estimation through cloud analysis (Jalayer et al., 2015).

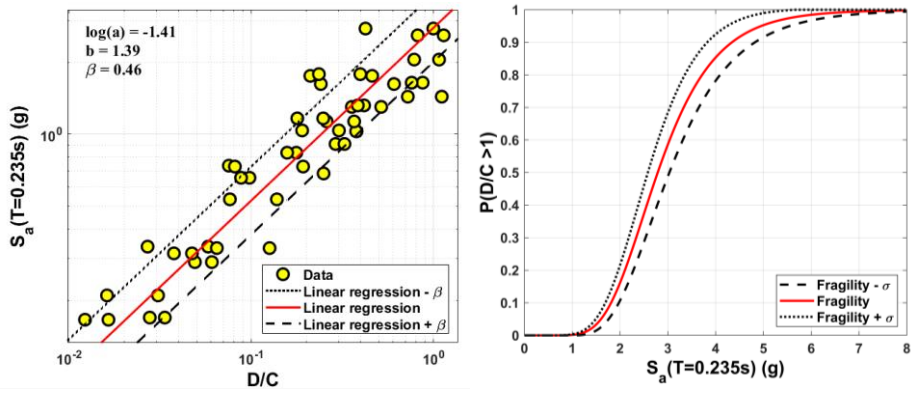

Figure 11. (a) Linear regression of pounding against the spectral acceleration. (b) Fragility curve for pounding.

Conclusions

This study used a non-linear finite element model of a template school that has been built by Pahar Trust across Nepal. This design had a 102 mm seismic gap as to avoid structural torsion that could have been created due to the non-symmetrical stiffness caused by the staircase. A modal analysis was carried out as to identify which mode of vibration caused lateral displacement across the seismic gap. Three ground motions sets were then collated, set 1 was formed of 5 pairs of recordings from the 2015 Gorkha earthquake, set 2 was formed of 11 pairs of recordings which were Eurocode compliant with a PGA of 0.38 g and set 3 were the same ground motions as set 2 but with a scaling factor of 1.58 resulting in a PGA of 0.60 g. NLTHA was then carried out as to assess the interstorey drift and effectiveness of the seismic gap. Finally, fragility analysis was carried out using the linear regression approach for cloud analysis.

From the results of the fragility analysis we can see that the structure can be considered safe as it has a 50% probability of pounding at 2.7 g. The interstorey drift levels for the two structures exceed the Eurocode threshold for nonstructural brittle elements for the post-Gorkha PSHA ground motion set. For the pre-Gorkha ground motion set the median value interstorey drift was 0.59% and 0.70% for building 1 and building 2 respectively hence they also exceed the threshold for non-structural brittle elements. The levels of interstorey drift do not exceed the 0.5% Eurocode threshold for any of the Gorkha 2015 ground motions.

Further work could be carried out looking at the damage incurred by the structures that were completed prior to the 2015 Gorkha earthquake. Furthermore, the structural impact of the masonry infill could be investigated. Fragility analysis could be carried out for a variety of limit states to evaluate the effects of an earthquake outside of pounding.

Acknowledgements

This work was funded by the Engineering and Physical Science Research Council (EPSRC) under the project “Seismic Safety and Resilience of Schools in Nepal” SAFER (EP/P028926/1). Further information available at http://www.safernepal.net/.

References

Bommer, J. and Acevedo, A. (2004). The Use of Real Earthquake Accelerograms as Input to Dynamic Analysis. *Journal of Earthquake Engineering*, 8(sup001), pp.43-91.

Catlos, E., Friedrich, A., Lay, T., Elliot, J., Carena, S., Upreti, B., DeCelles, P., Tucker, B. and Bendick, R. (2016). Nepal at Risk: Interdisciplinary Lessons Learned from the April 2015 Nepal (Gorkha) Earthquake and Future Concerns. *GSA Today*, 26(06), pp.42-43.

Chaulagain, H., Rodrigues, H., Silva, V., Spacone, E. and Varum, H. (2015). Seismic risk assessment and hazard mapping in Nepal. *Natural Hazards*, 78(1), pp.583-602.

EN 1998-1 (2004). Eurocode 8: Design of structures for earthquake resistance - Part 1 : General rules, seismic actions and rules for buildings [Ebook] (1st ed.). Brussels: BSi.

EN 1998-1-1. (2004). Eurocode 2: Design of concrete structures - Part 1-1 : General rules and rules for buildings [Ebook] (1st ed.). Brussels: BSi.

EN 1998-3. (2005). Eurocode 8: Design of structures for earthquake resistance - Part 3: Assessment and retrofitting of buildings [Ebook] (1st ed.). Brussels: BSi.

Fardis, M. (2009). *Analysis and Modelling for Seismic Design or Assessment of Concrete Buildings*. 1st ed. Dordrecht: Springer, p.362.

Favvata, M. (2017). Minimum required separation gap for adjacent RC frames with potential inter-story seismic pounding. *Engineering Structures*, 152, pp.643-659.

Filippou F.C., Popov, E.P., and Bertero, V.V. (1983). "Effects of Bond Deterioration on Hysteretic Behavior of Reinforced Concrete Joints". Report EERC 83-19, Earthquake Engineering Research Center, University of California, Berkeley.

Ghimire, S. and Parajuli, H. (2016). Probabilistic Seismic Hazard Analysis of Nepal considering Uniform Density Model. *Proceedings of IOE Graduate Conference*, pp.115-122.

Jalayer, F., De Risi, R. and Manfredi, G. (2015). Bayesian Cloud Analysis: efficient structural fragility assessment using linear regression. Bulletin of Earthquake Engineering, 13(4), pp.1183-1203.

Karayannis, C. and Favvata, M. (2004). Earthquake-induced interaction between adjacent reinforced concrete structures with non-equal heights. *Earthquake Engineering & Structural Dynamics*, 34(1), pp.1-20.

Kent, D. C., and Park, R. (1971), "Flexural members with confined concrete". Journal of the Structural Division, 97(7), 1969-1990

Kolozvari K., Orakcal K., and Wallace J. W. (2015). "Shear-Flexure Interaction Modeling of reinforced Concrete Structural Walls and Columns under Reversed Cyclic Loading", Pacific Earthquake Engineering Research Center, University of California, Berkeley, PEER Report No. 2015/12

Lin, J. and Weng, C. (2001). Probability analysis of seismic pounding of adjacent buildings. *Earthquake Engineering & Structural Dynamics*, 30(10), pp.1539-1557.

Menegotto, M., and Pinto, P.E. (1973). Method of analysis of cyclically loaded RC plane frames including changes in geometry and non-elastic behavior of elements under normal force and bending. Preliminary Report IABSE, vol 13.

Mugnier, J., Huyghe, P., Gajurel, A., Upreti, B. and Jouanne, F. (2011). Seismites in the Kathmandu basin and seismic hazard in central Himalaya. *Tectonophysics*, 509(1-2), pp.33-49.

Mulargia, F., Stark, P. and Geller, R. (2017). Why is Probabilistic Seismic Hazard Analysis (PSHA) still used?. *Physics of the Earth and Planetary Interiors*, 264, pp.63-75.

Pahar Trust. 2019. *Personal communication with Flavia De Luca*, 18 February.

Pahar-trust.org. (2019). *Pahar Trust Nepal*. [online] Available at: https://www.pahar-trust.org/ [Accessed 17 Apr. 2019].

Park, R., Priestley, M. J. N., and Gill, W. D. (1982), "Ductility of square-confined concrete columns". Journal of the Structural Division, 108, 929-950.

Paudyal, Y., Yatabe, R., Bhandary, N. and Dahal, R. (2012). A study of local amplification effect of soil layers on ground motion in the Kathmandu Valley using microtremor analysis. *Earthquake Engineering and Engineering Vibration*, 11(2), pp.257-268.

Pokhrel, R. M., De Risi, R., Werner, M. J., De Luca, F., Vardanega, P. J., Maskey, P. N., & Sextos, A. (2019). Simulation-based PSHA for the Kathmandu Basin in Nepal. Proceeding of the 13 International Conference on of Applications of Statistics and Probability in Civil Engineering, 26-30 May, Seoul, South Korea.

Rajaure, S., Asimaki, D., Thompson, E., Hough, S., Martin, S., Ampuero, J., Dhital, M., Inbal, A., Takai, N., Shigefuji, M., Bijukchhen, S., Ichiyanagi, M., Sasatani, T. and Paudel, L. (2016). Characterizing the Kathmandu Valley sediment response through strong motion recordings of the 2015 Gorkha earthquake sequence. *Tectonophysics*, 714-715, pp.146-157.

Ram, T. and Wang, G. (2013). Probabilistic seismic hazard analysis in Nepal. *Earthquake Engineering and Engineering Vibration*, 12(4), pp.577-586.

Rupakhety, R., Olafsson, S. and Halldorsson, B. (2017). The 2015 Mw 7.8 Gorkha Earthquake in Nepal and its aftershocks: analysis of strong ground motion. *Bulletin of Earthquake Engineering*, 15(7), pp.2587-2616.

Scott, M. and Fenves, G. (2006). Plastic Hinge Integration Methods for Force-Based Beam–Column Elements. *Journal of Structural Engineering*, 132(2), pp.244-252.

Skrekas, P., Sextos, A. and Giaralis, A. (2014). Influence of bi-directional seismic pounding on the inelastic demand distribution of three adjacent multi-storey R/C buildings. *Earthquakes and Structures*, 6(1), pp.71-87.

Stevens, V., Shrestha, S. and Maharjan, D. (2018). Probabilistic Seismic Hazard Assessment of Nepal. *Bulletin of the Seismological Society of America*, 108(6), pp.3488-3510.

Appendix

Earthquake	Station	Orientation	Year	Vs30 (m/s)	Rjb (km)	M_w
Chi-Chi, Taiwan	TCU084	000, 090	1999	665.2	0	7.6
Christchurch, New Zealand	Hulverstone Drive Pumping Station	266, 356	2011	206	4.32	6.2
Chuetsu-oki, Japan	Nagaoka	000, 090	2007	514.3	3.97	6.8
Gazli, USSR	Karakyr	000, 090	1976	259.59	3.92	6.8
Loma, Prieta	LGPC	000, 090	1989	594.83	0	6.9
Mammoth Lakes 01	Long Valley Dam	000, 090	1980	537.16	12.56	6.1
Manjil, Iran	Abbar	000, 090	1990	723.95	12.55	7.4
Parkfield-02, CA	Parkfield - Fault Zone 14	000, 360	2004	246.07	8.45	6.0
St Elias, Alaska	Icy Bay	090, 180	1979	306.37	26.46	7.5
Tottori, Japan	TTRH02	000, 090	2000	310.21	0.83	6.6
Westmorland	Westmorland Fire Station	090, 180	1981	193.67	6.18	5.9

Table 2: summary of code conforming ground motions from PEER NGA West-2

Station	Orientation	Latitude	Longitude	Location
KATNP	000, 090	27.71307	85.3161	Kanti Path
KTP	230, 320	27.68182	85.27261	Kirtipur Municipality Office
THM	090, 180	27.68072	85.3772	University Grant Commission Office, Bhaktapur
TVU	000, 090	27.68145	85.28821	Central Department of Geology
PTN	090, 360	27.68082	85.31897	Engineering College, Pulchowk

Table 3: Summary of Gorkha 2015 ground motion recordings.